Volume 13 | Number 16 | 28 April 2017 | Pages 2895–3062

Soft Matter

rsc.li/soft-matter-journal

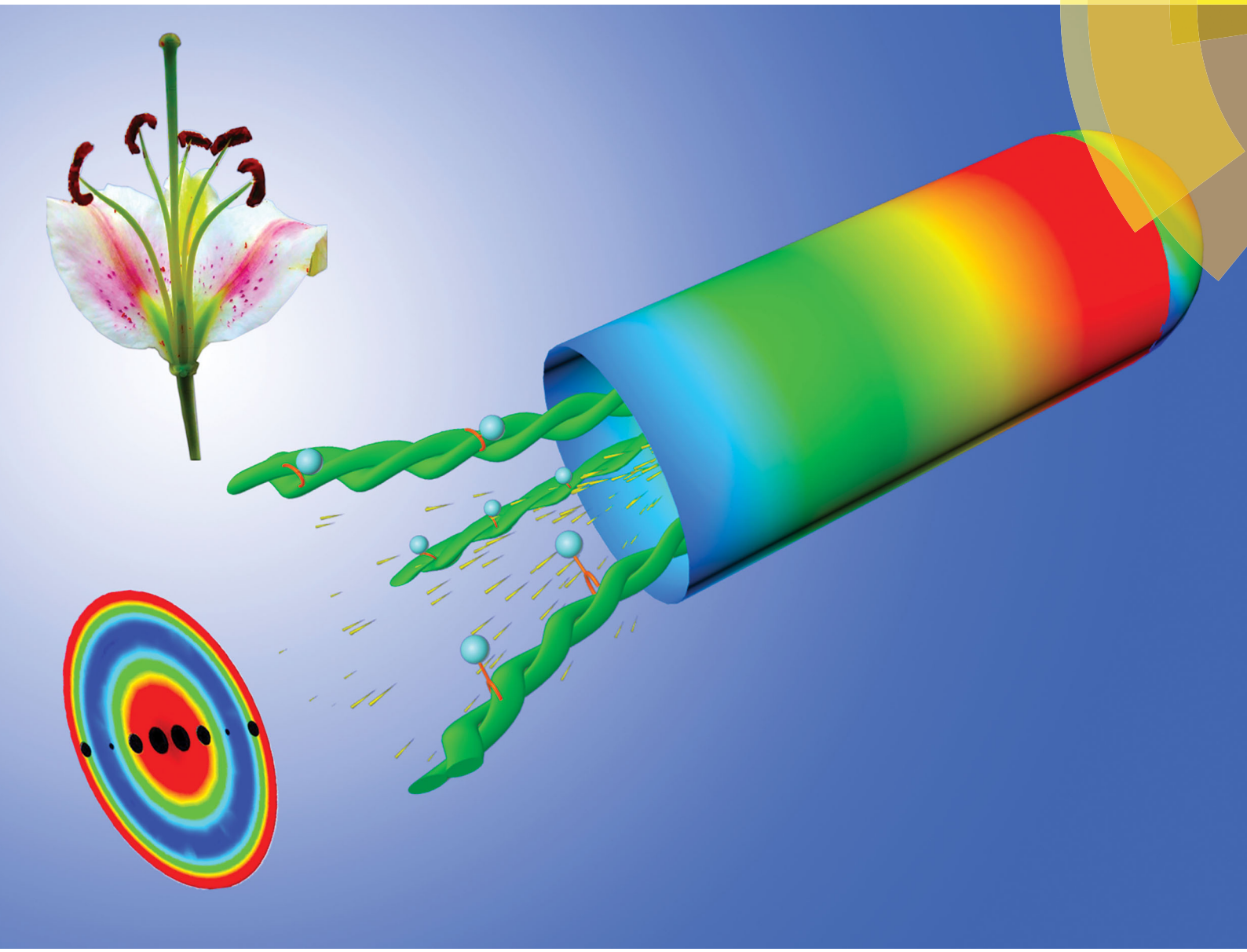

ISSN 1744-6848

ROYAL SOCIETY OF CHEMISTRY

PAPER

Feng Xu, Tian Jian Lu *et al.*

Fountain streaming contributes to fast tip-growth through regulating the gradients of turgor pressure and concentration in pollen tubes

Soft Matter

PAPER

View Article Online
View Journal | View Issue

Cite this: *Soft Matter*, 2017, 13, 2919

Fountain streaming contributes to fast tip-growth through regulating the gradients of turgor pressure and concentration in pollen tubes†

ShaoBao Liu,‡[ab] Han Liu,‡[bc] ShangSheng Feng,[ab] Min Lin,[bc] Feng Xu*[bc] and Tian Jian Lu*[ab]

Received 18th August 2016,
Accepted 27th February 2017

DOI: 10.1039/c6sm01915c

rsc.li/soft-matter-journal

Fountain streaming is a typical microfluidic pattern in plant cells, especially for cells with a high aspect ratio such as pollen tubes. Although it has been found that fountain streaming plays crucial roles in the transport of nutrients and metabolites, the positioning of organelles and the mixing of cytoplasms, its implications for the fast tip growth of pollen tubes remain a mystery. To address this, based on the observations of asiatic lily *Lilium Casablanca*, we developed physical models for reverse fountain streaming in pollen tubes and solved the hydrodynamics and advection–diffusion dynamics of viscous Stokes flow in the shank and apical region of pollen tubes. Theoretical and numerical results demonstrated that the gradients of turgor pressure and concentration of wall materials along the length of pollen tubes provide undamped driving force and high-efficiency materials supply, which are supposed to contribute to the fast tip-growth of pollen tubes. The sample experimental results show that the tip-growth will be abnormal when the gradients of turgor pressure change under osmotic stress induced by different concentrations of PEG-6000 (a dehydrant).

1. Introduction

Cytoplasmic streaming, also called cyclosis, is a movement of cytoplasms in various organisms varying from bacteria to higher plants and animals.[1,2] This motion assists in the delivery of nutrients, metabolites, organelles and other materials to all parts of the cell.[3–5] Several observations indicate that cytoplasmic streaming plays important roles in various biological processes, such as fast tip-growth of pollen tubes and root hairs,[6,7] movement of chloroplasts in plant cells,[8] asymmetric positioning of meiotic spindles in mammalian embryos,[9] and developmental potential of zygote.[10,11] Different flow patterns in plant cells have been found, such as "fountain" streaming (with motion near the central axis of the cell opposite to that at the periphery) in *lily* pollen tubes,[4] and spiral "rotational" streaming in *Chara*.[4,5] Among these patterns, "fountain streaming" has attracted special attention due to its important role in longitudinal transportation along plant cells, especially for cells with a high aspect ratio such as pollen tubes, root hairs and fungus hypha.[6,7,12] In spite of its important roles, the implications of fountain streaming for the fast tip-growth of pollen tubes remain a mystery.[13] In this paper, taking reverse fountain flow as an example, we investigated the roles of fountain streaming in the fast tip-growth of pollen tubes.

Fountain streaming is commonly found in pollen tubes, which is the cellular protuberance formed by the male gametophyte in angiosperm species delivering sperm to the ovary of the receptive flower to perform double fertilization. Pollen tubes exhibit an extremely high aspect ratio with the length of the cell (~2 mm) measuring up to hundred times its diameter (~20 μm). Fountain streaming in pollen tubes, similar to the cytoplasmic streaming in other plant cells, may have at least three important functions: the transport of nutrients and metabolites, the positioning of organelles, and the generation of convection for enhanced chemical and enzymatic reactions.[3] Of significant importance is the fountain streaming in pollen tubes. Fountain streaming continuously provides the driving force for the tip growth and transports cell wall materials over a huge distance in a highly efficient and targeted manner. The growth rate of pollen tubes at up to 0.6 mm h^{-1} (the fastest growing plant cell types known) is rather impressive, given that the growth speed is a direct competitive selection factor for the success of fertilization.[14] It has been known that the turgor

[a] State Key Laboratory for Strength and Vibration of Mechanical Structures, School of Aerospace, Xi'an Jiaotong University, Xi'an 710049, P. R. China. E-mail: tjlu@mail.xjtu.edu.cn
[b] Bioinspired Engineering and Biomechanics Center (BEBC), Xi'an Jiaotong University, Xi'an 710049, P. R. China. E-mail: fengxu@mail.xjtu.edu.cn
[c] MOE Key Laboratory of Biomedical Information Engineering, School of Life Science and Technology, Xi'an Jiaotong University, Xi'an 710049, P. R. China

† Electronic supplementary information (ESI) available. See DOI: 10.1039/c6sm01915c

‡ Co-first authors: they contributed equally to this work.

pressure and the distribution of wall materials (*e.g.*, ions, vesicles) in the pollen tube contribute to its growth. This is because the turgor pressure generates the mechanical stress leading to the expansion of the cell wall,[15] while the distribution of wall materials controls the deposition of new materials into the synthetic wall for pollen tube elongation, navigation and self-incompatibility response.[16] For example, the well-known Lockhart equation[15,17] states that the rate of cell wall expansion is proportional to the difference between the turgor pressure and a critical threshold value. The gradient of Ca^{2+} concentration in pollen tubes drops off sharply from around 1–5 μm at the apex of a growing tube to basal values of 150–300 nm within 20 μm and the disruption of this gradient causes cessation of pollen tube growth.[16] Although these pieces of evidence show that the turgor pressure and concentration gradient are correlated with pollen tube growth, it remains elusive how the hydrodynamics and intracellular transportation contribute to the fast tip-growth of pollen tubes.

Recently, some theoretical analyses have been proposed to explore the underlying mechanism of the functions of cytoplasmic streaming in plant and animal cells. For instance, Goldstein *et al.*[4,18] found strongly enhanced lateral transport and longitudinal homogenization by solving the dynamics of fluid flow and diffusion for the archetypal "rotational streaming" (in *Chara* and *Nitella*). In migrating cells, cytoplasmic streaming enhances the transport of actin monomers in the direction of cell movement.[19,20] At one-cell stage of the Caenorhabditis elegans embryo, cortical flow transports proteins (*e.g.*, PAR-3, PAR-6, and PKC-3) that are essential for cell polarity toward the anterior. Thus cortical flow contributes to the establishment of anterior–posterior polarity of the embryo.[9,21,22] Regarding early Drosophila embryos, cytoplasmic streaming has been shown to improve the scale of the bicoid morphogen gradient and affect the position-dependent differentiation.[11] In spite of all these efforts, it remains elusive how the fountain streaming generates the turgor pressure gradients in fast tip-growing pollen tubes and how the fountain streaming regulates the distribution of wall materials.

Here, motivated by the phenomenology of asiatic lily *Lilium Casablanca* (Fig. 1a), this study proposes mathematical models to provide insights into the previously asked questions by examining the most basic aspects of fountain streaming flows. The aim of this study is to illustrate how fountain streaming contributes to the fast tip-growth of pollen tubes in terms of driving force and materials supply. To this end, mathematical models of hydrodynamics and advection–diffusion dynamics for fountain streaming have been developed. Theoretical and numerical results demonstrate the enhancement of turgor pressure and concentration of cell wall synthesis materials at the apical region, both of which are correlated directly with the fountain geometry of flow. The roles of fountain streaming in fast tip-growing pollen tubes are examined by disordering the hydrodynamics through applying the osmotic stress *in vitro*.

2. Materials and methods

2.1. Pollen collection, germination and osmotic stress

In the experiment, the mature anthers of asiatic lily *Lilium Casablanca* were packed and placed in a Petri dish. The scattered pollen grains at the bottom of the Petri dish were collected and stored in a centrifugal tube at −70 °C. Silicone balls were applied in the Petri dish and centrifugal tube for drying. To observe the cytoplasmic streaming in pollen tubes, the pollen grains were first thawed in a moist chamber for ∼10 hours at 4 °C and 2 h at room temperature in the moist chamber, and then cultured in the medium (1.27 mM $CaCl_2$, 0.162 mM H_3BO_3, 0.99 mM KNO_3, 290 mM sucrose, pH 5.2) for germination for 3 hours.[23] PEG-6000 is a kind of dehydrant which changes the osmotic pressure out of the plant cell, and is often used for simulating

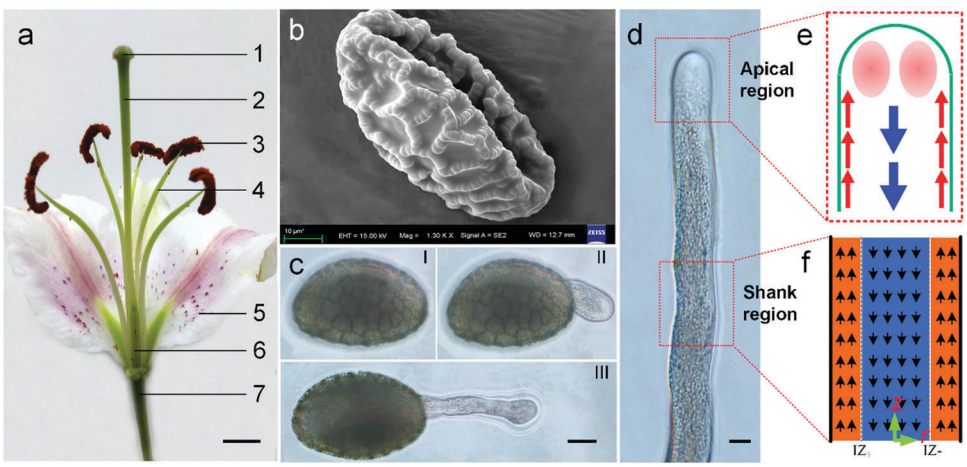

Fig. 1 Observations and simplified model of fountain streaming in pollen tubes. (a) A blooming asiatic lily *Lilium Casablanca* from Yunnan, China, with stigma (1), style (2), anther (3), filament (4), petal (5), ovule (6) and pedicel (7); (b) scanning electron microscopy image of a pollen grain; (c) microscope image of a fast tip-growing pollen tube, I (t = 0), II (t = 30 min) and III (t = 60 min); (d) fountain streaming in a pollen tube, shown as a movie (ESI,† Movie); (e) an idealized streaming pattern in the apical region of pollen tubes and (f) in the shank region with indifferent zones $IZ_{\pm}$ in a cylindrical coordinate. The scale bars are (a) 1 cm, (c) 20 μm, (d) 10 μm.

the drought conditions *in vitro*. To investigate the effects of turgor pressure on the tip-growth of pollen tubes, pollen grains were cultured under osmotic stress with different concentrations of PEG-6000 in the medium.

2.2. Living image and observation

Several different microscopes and camera were used for the characterization of pollen grains, pollen tubes and their cytoplasmic streaming. In the scanning electron microscope (SEM), the pollen grain appears as a cage (Fig. 1b). Fig. 1a has been obtained using a camera Nikon D90, and Fig. 1b has been obtained using an ultra-high resolution field emission scanning electron microscope (SEM), ZEISS MERLIN Compact. After being cultured for a period of time, the pollen grain started germinating, and a tube protruded from the pollen grain and elongation was accompanied by fast tip-growth (Fig. 1c). The obvious fountain streaming in the fast tip-growing pollen tube was observed (Fig. 1d) on a research level inverted microscope, the Olympus IX81. Whereas images and SI Movie were recorded using a charge-coupled device (CCD) camera mounted on the research level inverted microscope Olympus IX81.

2.3. Hydrodynamics of fountain streaming

In order to simplify the theoretical description of the streaming in the pollen tube, biological complexities (*e.g.*, geometry defects, tonoplast, distinction between the cytoplasm and the vacuole) can be stripped away. When this is done, the structure can be simplified to the idealized geometry represented by a cylinder of a long distance shuttling region (Fig. 1e) and an apical tip of a short distance targeting region (Fig. 1f). The viscous Stokes equation was used for controlling the incompressible Newtonian fluid with velocity u and pressure p. In the long distance shuttling region, the theoretical results for the distribution of flow velocity and turgor pressure p were solved by using an analytical method (ESI†) and the numerical results were solved by using a commercial software (COMSOL Multiphysics 4.4). In the short distance targeting region, the simulation of flow velocity and turgor pressure was performed on COMSOL Multiphysics 4.4. The parameters used in the simulation are shown in Table 1.

2.4. Advection–diffusion of fountain streaming

The intracellular transportation of fountain streaming for the species of cell wall materials in pollen tubes is a fascinating field of research, while there are currently only a few theoretical studies that offer the underlying details.[5] In this study, coupling the hydrodynamics and advection–diffusion, the numerical simulation was performed to investigate the concentration of cell wall materials and the gradient of concentration at the apical region of pollen tubes with a different Péclet number Pe. The Pe number is defined as the ratio of the time taken by organelles to diffuse *versus* the time taken by the organelles to be adverted across a certain distance (Pe = Lv/D, where L is a characteristic distance, v is the velocity of particles and D is the diffusion coefficient of the particles). The geometry of the model is a cylinder with an apical cap with the sliding velocity and flux boundary conditions. The simulation was performed on COMSOL Multiphysics 4.4. The parameters used in the simulation are shown in Table 1.

Table 1 Parameters of pollen tubes and the properties of hydrodynamics and mass transfer of fountain streaming

Physical quality	Value
Density (ρ)	10^3 kg m^{-3} (water)[19,24]
Dynamic viscosity (η)	10^{-3} kg m^{-1} s^{-1} (Pa s) (water)[19,24]
Diffusion constant (D)	10^{-9} m^2 s^{-1} (smallest molecules)[18] 10^{-13} to 10^{-9} m^2 s^{-1} (vesicle)[24] 6.25×10^{-13} m^2 s^{-1} (vesicle)[24]
Speed of cyclosis (U)	10^{-4} m s^{-1} (chara corallina)[18] 4.5×10^{-7} m s^{-1} (pollen tube)[24] 2–9 $\times 10^{-7}$ m s^{-1} (pollen tube)[25]
Radius (R)	5×10^{-4} m (chara corallina)[18] 6.5×10^{-6} m (*Lilium longiflorum* pollen tubes)[24] 10^{-5} m (pollen tube of lily, measuring) 7.5×10^{-8} m (vesicle)[24]
Péclet number $\left(\mathrm{Pe} = \frac{UR}{D}\right)$	50 (smallest molecules)[4,18] 500–1000 (larger proteins)[4,18] 100–1000[4,18] 0.054[24]
Reynolds number $\left(\mathrm{Re} = \frac{UR}{v}\right)$	2.9×10^{-6} (*Lilium longiflorum* pollen tubes)[24]
Turgor pressure (P)	0.1–0.4 MPa (pollen tube of lily)[20,26,27]
Growth rates (V_{Pole})	$\leq$20 μm h^{-1} (in gymnosperms)[26] 80 to 600 μm h^{-1} (in ancient angiosperm lineages)[14] 0.1–0.35 μm s^{-1}[26]

The local turgor pressure and concentration of species at the clear zone at the apex of pollen tubes may be influenced by massive water uptake and the local concentration may be affected by the vesicle absorption and fusion for wall material synthesis.[23] In order to highlight the critical roles of fountain streaming in the hydrodynamics and intracellular transport for the fast tip-growth of pollen tubes, we eliminated the interference factors (i.e., not considering the "sources" or "sinks") in the simulation.

3. Results and discussion

3.1. Hydrodynamics of fountain streaming in pollen tubes

Stripping away biological complexities (e.g., geometry defects, tonoplast, distinction between the cytoplasm and vacuole) of streaming in pollen tubes, we study the case of an ideal geometry, i.e., a cylinder of a long distance shuttling region (Fig. 1e) and an apical tip of a short distance targeting region (Fig. 1f), whose inner surface has the equivalent velocity boundary conditions ($u_z = \bar{u}_z$) although the cytoplasmic streaming emerges naturally by the microfilament self-organization when the myosin motors moving on the actin bundle track at the periphery. Considering that the Reynolds number is small in pollen tubes

(Re = 2.9 × 10^{-6}),[24] we neglected the terms involving the local inertia force, the inertia force of convection, and the body force. For an incompressible Newtonian fluid with velocity u ($\nabla \cdot u = 0$) and pressure p, the viscous Stokes equation is given by

$$\eta \nabla^2 u = \nabla p \tag{1}$$

where η is the dynamic viscosity (Pa s). If V_{Pole} is the growth rate of a pollen tube, the flux through its cross-section is given by

$$\int_0^R 2\pi r u_z \mathrm{d}r = V_{\mathrm{Pole}} \pi R^2 \tag{2}$$

For the region of long distance shuttling, disregarding the end effects and radial flow, the velocity components are $u_z = u_z(r)$ and $u_r = u_\theta(r) = 0$ and the pressure distribution is $p = p(z)$ in cylindrical coordinates. The velocity components automatically satisfy the incompressible condition of continuity equations. By solving the viscous Stokes equation (ESI†) and giving the hydrostatic pressure in pollen tube p_o (initial pressure), the dimensionless velocity distribution in the radial direction is given as:

$$\frac{u_z}{\bar{u}_z} = 1 - 2(1-\xi)\left(1 - \frac{r^2}{R^2}\right) \tag{3}$$

and the dimensionless pressure along the length is given by

$$\frac{p}{p_o} = 1 + \frac{8(1-\xi)}{\psi}\frac{z}{L} \tag{4}$$

where $\xi = V_{\mathrm{Pole}}/\bar{u}_z$ and $\psi = R^2 p_o/\eta L \bar{u}_z$. Each pollen tube inherently has a pair of dimensionless ratios ξ and ψ, which determine the hydrodynamic property of fluid flow in the pollen tube. Let eqn (3) equates to zero, we obtain the indifferent zone at $|r/R|_{\mathrm{IZ}} = 1/\sqrt{2(1-\xi)}$, at which a vesicle-free line separates apically and basipetally directed cytoplasmic streams.

To verify the above results, we numerically simulated the fluid flow in the shank region of pollen tubes by choosing a cylinder aspect ratio of 20 as a representative model of pollen tubes: a cylinder with a radius of 10 μm and a length of 200 μm (Fig. 2a). Although mature pollen tubes achieve a large aspect ratio of 100, it is reasonable to perform the numerical simulation in a cylinder with an aspect ratio of 20, because the streaming rates become independent of the cell length (L) if the aspect ratio is more than 5 ($L > 5R$).[28] The sliding velocity $\bar{u} \sim 10$ μm s^{-1} at $r = R$ and the slip boundary at either end are applied. The fluid flow is simplified as viscous Stokes flow controlled by eqn (1). The 3D view and lateral view of the velocity field of the fountain streaming are presented in Fig. 2b and c. An inverse fountain flow is presented at the tip of the pollen tube: forward from the end to the tip in the inner region and backward from the tip to the end in the outer region. To obtain velocity distribution at the radial direction, we took a section view of the velocity field at the middle position, where the end effect is negligible (Fig. 2d). A parabolic velocity along the diameter of the pollen tube shows good agreement with the analytical solution of eqn (3) (Fig. 2e).

The cytoplasmic streaming in the algae (*e.g.*, cross-sectional velocity distribution) has been characterized in detail through both experimental measurement and numerical simulation.[18,29] There are few experimental data for streaming velocity in pollen tubes. To ensure the reliability of the simulated results, the velocity of cytoplasmic streaming in *characean algae* was firstly

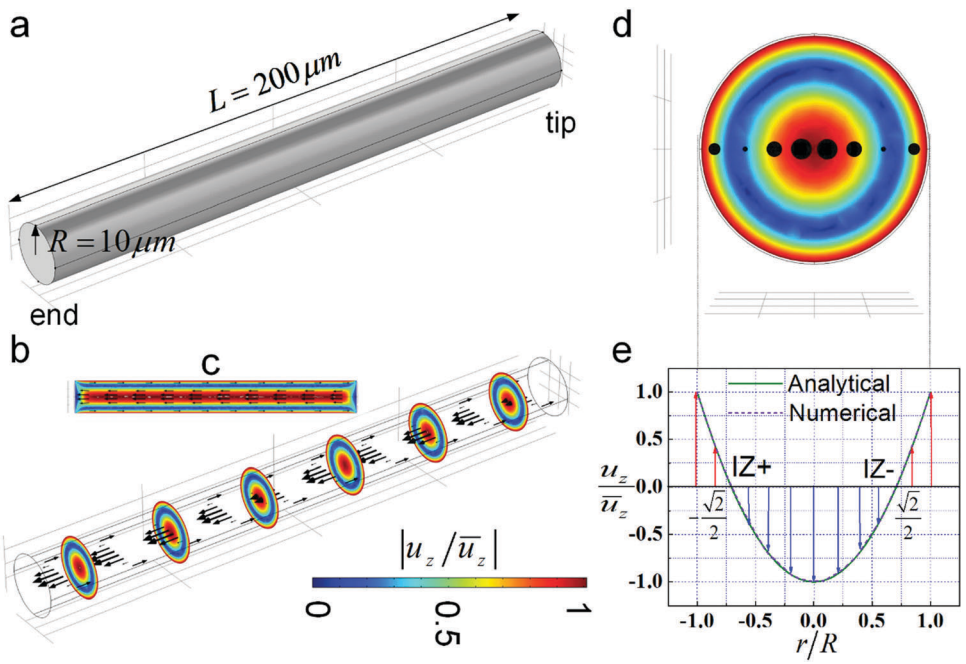

Fig. 2 Hydrodynamics of fountain streaming in the shank region of pollen tubes. (a) Simplified geometry for the shank region of pollen tubes; (b) 3D section slides of velocity field; (c) slide view of the velocity field; (d) section view of the velocity field; (e) comparison with the numerical and analytical velocity along a diameter of pollen tubes.

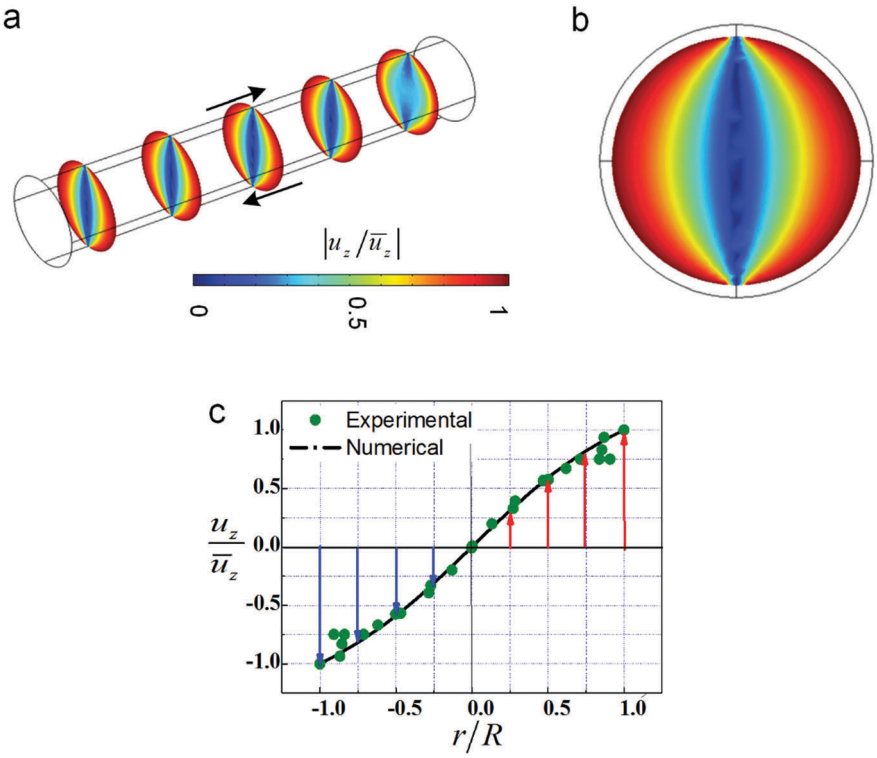

Fig. 3 Comparison of numerical and experimental hydrodynamics in characean algae cell. (a) 3D section slides of velocity field; (b) section view of the velocity field; (c) comparison of the numerical velocity along the diameter with the experimental results of ref. 29.

reconstructed using a similar method reported in the literature.[18,30] The case of $V_{\mathrm{Pole}} = 0$ was investigated by setting the velocity boundary conditions to those used in ref. 18, except for the helicity of the flow. The 3D section slides of the velocity field (Fig. 3a) as well as its section view (Fig. 3b) are asymmetric. And the cross-sectional velocity distribution well reconstructed the sigmoidal velocity distribution experimentally observed *in vivo* (Fig. 3c, green dots).[29] This suggests that the numerical method proposed here is capable of simulating fountain streaming in pollen tubes.

In the case of a lily pollen tube, the growth rate of the pollen tube is $V_{\mathrm{Pole}} \sim 10^{-3}$ to 10^{-1} μm s^{-1} and the maximum velocity of fluid flow is $\bar{u} \sim 10^{-1}$ to 1 μm s^{-1} (Table 1), so the ratio ξ is in the range of 10^{-2} to 10^{-1}. In the case of $\xi = 0$, the resulting dimensionless velocity distribution $u_z/\bar{u}_z \approx 1\text{–}2(1 - r^2/R^20)$ and the resulting indifferent zone $|r/R|_{\mathrm{IZ}} = \sqrt{2}/2$ together imply a stable geometry of fluid flow in the pollen tube. As for the case when the pollen tube radius is on the order of $R \sim$ 1–10 μm, the pollen tube has a length on the order of $R \sim 1\text{–}10^3$ μm, the initial pressure of the pollen tube is on the order of $p_{\mathrm{o}} \sim 10^{-1}$ MPa, the dynamic viscosity is on the order of $\eta \sim 10^{-3}$ to 10^{-2} Pa s, and the ratio ψ falls in the range of 10^4 to 10^{11}. Therefore, the dimensionless gradient of turgor pressure $8(1 - \xi)/\psi \sim 10^{-10}$ to 10^{-3} is small and negligible, making $p/p_{\mathrm{o}} \approx 1$. However, in the abnormal cases (*e.g.*, under osmotic stress), the gradient of turgor pressure will increase when the initial pressure p_{o} decreases because ψ becomes smaller with decreasing p_{o} when the pollen tubes are subjected to osmotic stress.

To illustrate the roles of fountain streaming in regulating the gradients of turgor pressure, the turgor pressure distribution can be calculated along the length of the pollen tubes. Under normal conditions (initial pressure $P_0 \sim 1$ MPa), the turgor pressure increases linearly along the length of the pollen tubes with a small gradient (Fig. 4a), which is opposite to that of an ordinary pipe with natural pressure drop due to the energy loss according to the Darcy–Weisbach equation.[30] In other words, the peculiar hydrodynamic properties of fountain streaming in pollen tubes continuously provide an undamped driving force *via* balancing the natural pressure drop. Under abnormal conditions (initial pressure $P_0 < 1$ MPa), the gradients of turgor pressure increase as the initial pressure decreases (Fig. 4b).

To investigate the influence of the pressure gradients on the tip-growth of pollen tubes, we observed the shape and rate of tip-growth of pollen tubes with different pressure gradients. The gradients of turgor pressure in a pollen tube are changed by adjusting the PEG-6000 concentration[31] *in vitro* (see details in Materials and methods). Compared with the control (no osmotic stress, Fig. 5a), the pollen tubes under the stress of 10% PEG-6000 grow with shorter and larger tips (Fig. 5b). The pollen tubes under the stress of 20% PEG-6000 further grow shorter and abnormally (Fig. 5c), while pollen tubes cannot germinate under the stress of 30% PEG-6000.

The experimental results suggest that the tip growth of pollen tubes is regulated by the gradient of turgor pressure. We tried to qualitatively interpret the regulation mechanisms of turgor pressure. Although the longitudinal array of actin microfilaments is deemed

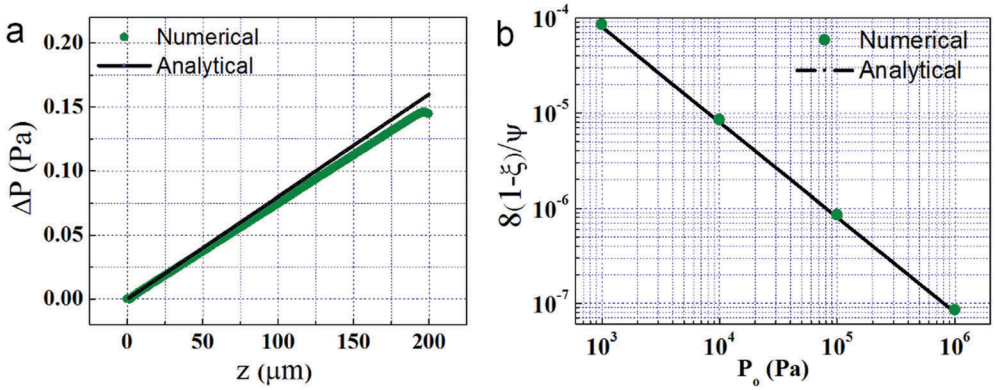

Fig. 4 Turgor pressure in pollen tubes and its effect on the shape of growing tip of pollen tubes. (a) The analytical and numerical turgor pressure linearly changes along the length of pollen tubes and the insertion is the numerical contours of turgor pressure; (b) the analytical and numerical gradient of the turgor pressure along the length of pollen tubes changes with the initial pressure.

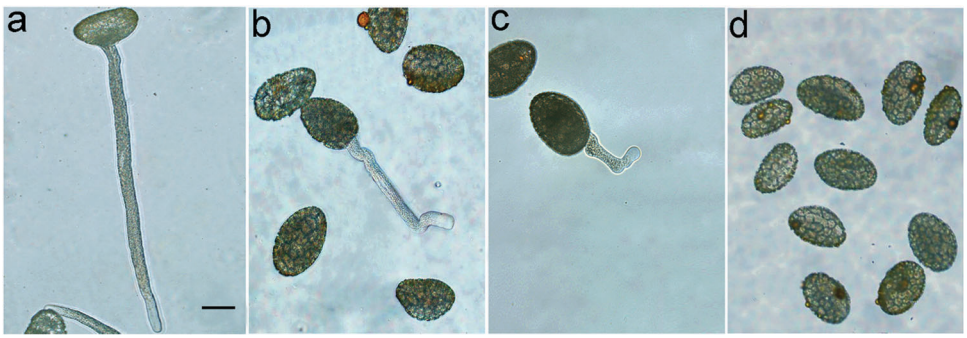

Fig. 5 Pollen tube growth under osmotic stress. (a) Control, no PEG-6000 (dehydrant) in the culture solution; (b) under the stress of 10% PEG-6000; (c) 20% PEG-6000; (d) 30% PEG-6000. The scale bar is 50 μm.

to drive the polar elongation of a pollen tube,[26] the turgor pressure provides the most important driving force for the fast tip-growth of pollen tubes.[32,33] According to Lockhart theory,[15,17] the rate of cell wall expansion is proportional to the difference between the actual turgor pressure and a threshold pressure. Thus a normal pollen tube (no osmotic stress), on one hand, has a relatively high tip-growth rate driven by a relatively high turgor pressure and on the other hand, maintains its elongation through the fountain streaming balancing the natural pressure drop and keeping an undamped driving force (without a significant decrease), as per the previous theoretical predictions. However, when the pollen tube is under osmotic stress, the gradients of turgor pressure will increase and may affect tip-growth of the pollen tube due to the decreased initial turgor pressure.

3.2. Intracellular transportation of fountain streaming in pollen tubes

Another critical factor for the fast tip-growth of a pollen tube is materials supply for cell wall synthesis, which mostly depends on the intracellular transportation of fountain streaming in pollen tubes. The movement of species of cell wall materials in pollen tubes is a fascinating example, but there is little theoretical understanding of the details.[5] An initial study of the interplay between calcium gradients and cytoplasmic streaming[34] provides an important step in unraveling the competition between advective and diffusional transportation of ions and microscopic particles in the tip-growth of plant cells. In this simulation, we investigated the advection–diffusion dynamics of viscous Stokes flow of fountain streaming in the apical region of pollen tubes. To estimate whether advection or diffusion is the dominant transport mode for inclusive microscopic particles (*e.g.*, ions, small molecules, vesicles or organelles) in fountain streaming, we first calculated the Péclet number (Pe) (defined in Materials and methods). Here, we take medium sized inclusions – vesicles as an example with the characteristic distance such as the tip radius of L = 10 μm, the vesicle velocity (v) of the order of 0.3–0.6 μm s^{-3}, and the diffusion coefficient of the vesicles D = 0.6 μm^2 s^{-1}.[24] The Péclet number Pe can be estimated to be in the range of 5–10, indicating that both diffusion and advection have a significant contribution to vesicle movement. For smaller species (*e.g.*, ions, small molecules) across smaller length scales (short-distance targeting region), the Péclet number Pe is small and hence diffusion will become more dominant. In contrast, for larger species (*e.g.*, large proteins, vesicles and organelles) across larger length scales (long-distance shutting region), the Péclet number Pe is large so that advection will become dominant. The advection–diffusion dynamics for the moving species in pollen tubes can be described by concentration C. The time-dependent concentration of a species due to diffusion

and cytoplasmic flow of fountain streaming can be generally described as

$$\frac{\partial C}{\partial t} = -u \cdot \nabla C + D\nabla^2 C + R \quad (5)$$

where D is the diffusion coefficient and u is the flow velocity. The term on the left hand side of this equation is the change in the species concentration for mass transfer. On the right hand side of this equation, the 1st term is the mass advection; the 2nd term is the mass diffusion and the last term represents any phenomena that act as mass "sources" or "sinks". Considering a constant growth rate under normal conditions, the time-independent case can be assumed in the equilibrium state. Neglecting any sources of ion channels localized at the tip of pollen tubes, the steady-state version is

$$D\nabla^2 C = u \cdot \nabla C \quad (6)$$

The simulation of advection–diffusion dynamics in the shank region of the pollen tube was performed by using an axisymmetric geometry with boundary conditions of the sliding velocity and flux (Fig. 6a), where the position of sliding velocity at the cell wall is based on the distribution of microfilaments in the pollen tube.[24,35] In the simulation, the normalized system parameters of inlet concentration ($\bar{C}$ = 1) and boundary flux (γ = 0.1) were used. The section slides of the normalized flow velocity show the pattern of inverse "fountain" (forward motion near the central axis of the cell and backward motion near the periphery) near the tip (Fig. 6b). This is consistent with the experimental observations (ESI,† Movie). To reveal the role played by "fountain" streaming in regulating the materials supply for fast tip-growth, we investigated the influence of Péclet numbers on the distribution of concentration (Fig. 6c). Firstly, sharp patterns of concentration distribution appear at high Péclet numbers (Pe = 10^2 to 10^3), which indicates that the fountain streaming accumulates the materials for cell wall synthesis near the tip of pollen tubes. However, the pattern at medium Péclet numbers (Pe = 4–10, around the previously estimated range) becomes obtuse and reconstructs the spatial configuration of the inversely apical cone in experimental observations.[24,36] At low Péclet numbers (Pe = 1–2), the concentration distribution tends to be uniform in the apical pollen tube. These results indicate that the fountain streaming plays crucial roles in the distribution of cell wall materials, especially for the small species with medium and higher Péclet numbers.

To quantify the effects of fountain streaming on materials accumulation, we present the normalized concentration along the symmetry axis of the pollen tube for selected Péclet numbers (Fig. 6d). Interestingly, the styles of concentration distribution are very different at different Péclet numbers. At low Péclet numbers (Pe = 1–2), the concentration increases with a gentle slope from the end to the tip. At high Péclet numbers (Pe = 10^2 to 10^3), the concentration distribution increases exponentially which agrees with the previously mentioned Ca^{2+} concentration distribution.[16] In addition, the gradients of the concentration distribution along the symmetry axis of pollen tubes increase when the Péclet numbers become larger (Fig. 6e), indicating that materials accumulation is more efficient at higher Péclet numbers.

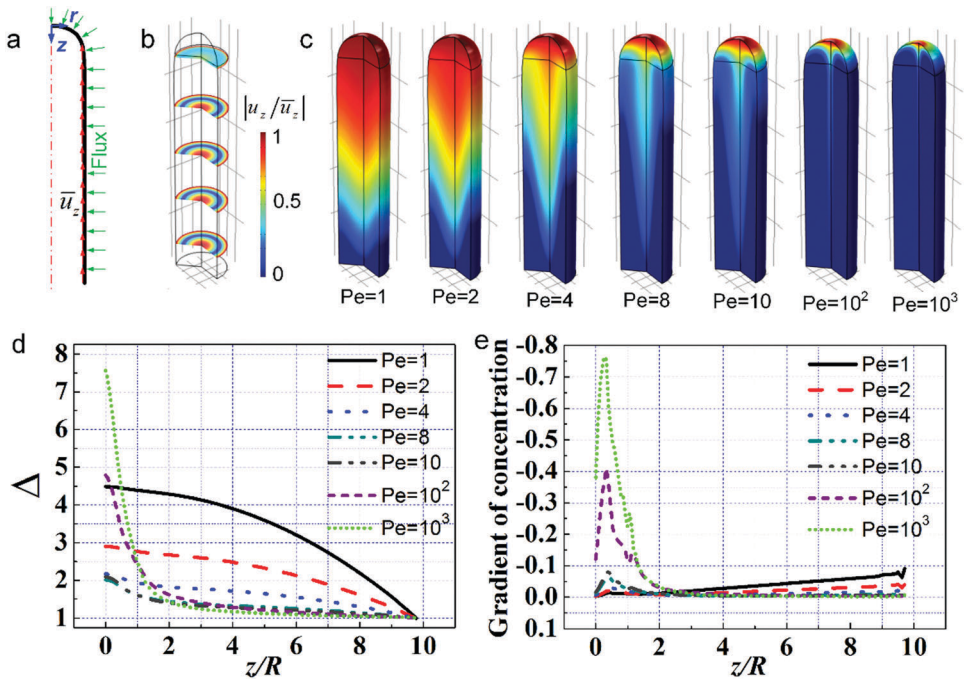

Fig. 6 Concentration in the apical region of pollen tubes. (a) The axisymmetric geometry and boundary conditions of the sliding velocity and flux; (b) the section slides of the normalized fluid velocity; (c) the patterns of normalized concentration with different Péclet numbers; (d) the normalized concentration along the axis of symmetry of pollen tubes with different Péclet numbers; (e) the gradient of concentration along the axis of symmetry of pollen tubes with different Péclet numbers.

Although ion channels localized at the tip of the pollen tube can generate the internal gradient of ions, the fountain streaming might be another mechanism contributing to the transportation and accumulation of cell wall materials (*i.e.*, ions, molecules and vesicles) for the fast tip-growth of pollen tubes. As is known, steep concentration gradients of cell wall materials are essential for polar cell growth.[37] In the apical pollen tube, both the calcium concentration of the cytoplasm as well as the pH value of the pollen tube change significantly over short distances.[16,38] This is because these ion gradients can not only provide the pollen tube a regulatory spatial framework for its polarity, but also involve in the temporal regulation of pollen tube elongation. In contrast, the disruption of the gradient invariably will cause cessation of pollen tube growth.[16] Given that the concentration gradient is necessary for fast tip-growth of pollen tubes, fountain streaming contributes to the fast tip-growth by regulating the supply of cell wall materials.

4. Conclusions

For flowering plants, pollen tubes are a catheter-like transport tool that serves to deliver the sperm cells from the pollen grain to the ovary of the receptive flower to perform double fertilization. This process is of critical importance for fast and polar tip-growth of the pollen tube. Both analytical and numerical methods introduced in this study provide an understanding of the roles of hydrodynamics and advection–diffusion of fountain streaming in fast-tip growing pollen tubes. These findings demonstrate that there are positive gradients of turgor pressure and concentration along the length of pollen tubes. Fountain streaming with unique properties of hydrodynamics and transportation generates an undamped driving force for the elongation of pollen tubes and also provides cell wall materials over huge distances in a highly efficient and targeted manner. These may be helpful for further understanding the sexual reproduction and infertility of flowering plants under normal conditions and drought stress.

Author contributions

T. J. L. and F. X. designed the research; S. B. L. and H. L. performed the research; S. B. L., M. L. and S. S. F. analyzed data; T. J. L., F. X., M. L., S. S. F., S. B. L. and H. L. wrote the paper.

Acknowledgements

This work was financially supported by the Major International Joint Research Program of China (11120101002), the National Natural Science Foundation of China (11372243), and Key Program for International S&T Cooperation Projects of Shaanxi (2013KW33-01). F. X. was also partially supported by the China Young 1000-Talent Program and the Program for New Century Excellent Talents in University. S. B. L. was supported by the China Scholarship Council to study as a visiting student at WUSTL.

References

1 R. E. Williamson and C. C. Ashley, *Nature*, 1982, **296**, 647–651.
2 W. E. Theurkauf, *Science*, 1994, **265**, 2093–2096.
3 Y. Chebli, J. Kroeger and A. Geitmann, *Mol. Plant*, 2013, **6**, 1037–1052.
4 J. W. Van De Meent, I. Tuval and R. E. Goldstein, *Phys. Rev. Lett.*, 2008, **101**, 178102.
5 J. Verchot-lubicz and R. E. Goldstein, *Protoplasma*, 2010, **240**, 99–107.
6 C. D. Justus, P. Anderhag, J. L. Goins and M. D. Lazzaro, *Planta*, 2004, **219**, 103–109.
7 T. Shimmen, *et al.*, *Protoplasma*, 1995, **185**, 188–193.
8 A. Kadota, *et al.*, *Proc. Natl. Acad. Sci. U. S. A.*, 2009, **106**, 13106–13111.
9 E. Munro, J. Nance and J. R. Priess, *Dev. Cell*, 2004, **7**, 413–424.
10 S. Ganguly, L. S. Williams, I. M. Palacios and R. E. Goldstein, *Proc. Natl. Acad. Sci. U. S. A.*, 2012, **109**, 15109–15114.
11 I. Hecht, W. J. Rappel and H. Levine, *Proc. Natl. Acad. Sci. U. S. A.*, 2009, **106**, 1710–1715.
12 L. J. Mckerracher and I. B. Heath, *Exp. Mycol.*, 1987, **11**, 79–100.
13 M. D. Lazzaro, E. Y. Marom and A. S. Reddy, *Planta*, 2013, **238**, 587–597.
14 J. H. Williams, *Proc. Natl. Acad. Sci. U. S. A.*, 2008, **105**, 11259–11263.
15 J. H. Kroeger, R. Zerzour and A. Geitmann, *PLoS One*, 2011, **6**, e18549.
16 T. L. Holdaway-clarke and P. K. Hepler, *New Phytol.*, 2003, **159**, 539–563.
17 J. A. Lockhart, *J. Theor. Biol.*, 1965, **8**, 264–275.
18 R. E. Goldstein, I. Tuval and J. W. Van De Meent, *Proc. Natl. Acad. Sci. U. S. A.*, 2008, **105**, 3663–3667.
19 K. Keren, *et al.*, *Nat. Cell Biol.*, 2009, **11**, 1219–1224.
20 M. Prass, K. Jacobson, A. Mogilner and M. Radmacher, *J. Cell Biol.*, 2006, **174**, 767–772.
21 S. Schonegg, A. T. Constantinescu, C. Hoege and A. A. Hyman, *Proc. Natl. Acad. Sci. U. S. A.*, 2007, **104**, 14976–14981.
22 R. Niwayama, K. Shinohara and A. Kimura, *Proc. Natl. Acad. Sci. U. S. A.*, 2011, **108**, 11900–11905.
23 L. C. Chang, *et al.*, *Plant Cell Physiol.*, 2009, **50**, 1558–1572.
24 J. H. Kroeger, F. B. Daher, M. Grant and A. Geitmann, *Biophys. J.*, 2009, **97**, 1822–1831.
25 A. Lovy-Wheeler, L. Cárdenas, J. G. Kunkel and P. K. Hepler, *Cell Motil. Cytoskeleton*, 2007, **64**, 217–232.
26 L. Vidali, S. T. Mckenna and P. K. Hepler, *Mol. Biol. Cell*, 2001, **12**, 2534–2545.
27 M. Pietruszka, *PLoS One*, 2013, **8**, e75803.
28 W. F. Pickard, *Protoplasma*, 1974, **82**, 321–339.
29 R. V. Mustacich and B. R. Ware, *Biophys. J.*, 1977, **17**, 229.
30 W. H. Tan and S. A. Takeuchi, *Proc. Natl. Acad. Sci. U. S. A.*, 2007, **104**, 1146–1151.
31 J. V. Lagerwerff, G. Ogata and H. E. Eagle, *Science*, 1961, **133**, 1486–1487.

32 R. Benkert, G. Obermeyer and F. W. Bentrup, *Protoplasma*, 1997, **198**, 1–8.
33 L. J. Winship, G. Obermeyer, A. Geitmann and P. K. Hepler, *Trends Plant Sci.*, 2011, **16**, 353–355.
34 M. D. Lazzaro, *et al.*, *J. Exp. Bot.*, 2005, **56**, 2619–2628.
35 J. Bove, *et al.*, *Plant Physol.*, 2008, **147**, 1646–1658.
36 L. Zonia and T. Munnik, *Trends Plant Sci.*, 2009, **14**, 318–327.
37 P. K. Hepler, L. Vidali and A. Y. Cheung, *Annu. Rev. Cell Dev. Biol.*, 2001, **17**, 159–187.
38 K. L. Wilsen, *et al.*, *Sex. Plant Reprod.*, 2006, **19**, 51–62.